

RSC Advances



This is an *Accepted Manuscript*, which has been through the Royal Society of Chemistry peer review process and has been accepted for publication.

Accepted Manuscripts are published online shortly after acceptance, before technical editing, formatting and proof reading. Using this free service, authors can make their results available to the community, in citable form, before we publish the edited article. This *Accepted Manuscript* will be replaced by the edited, formatted and paginated article as soon as this is available.

You can find more information about *Accepted Manuscripts* in the [Information for Authors](#).

Please note that technical editing may introduce minor changes to the text and/or graphics, which may alter content. The journal's standard [Terms & Conditions](#) and the [Ethical guidelines](#) still apply. In no event shall the Royal Society of Chemistry be held responsible for any errors or omissions in this *Accepted Manuscript* or any consequences arising from the use of any information it contains.

ARTICLE

Ionic liquids improve the anticorrosion performance of Zn-rich coatings

Cite this: DOI: 10.1039/x0xx00000x

M. Echeverría^{a*}, C. M. Abreu^a, F. J. Deive^b, M. A. Sanromán^b and A. Rodríguez^bReceived 00th January 2012,
Accepted 00th January 2012

DOI: 10.1039/x0xx00000x

www.rsc.org/

In this work, the suitability of the ionic liquid 1-ethyl-3-methyl imidazolium ethylsulfate ($C_2C_1imC_2SO_4$) for improving the anticorrosive behaviour of zinc rich paints (ZRP) has been demonstrated. The electrochemical performance of the coating has been evaluated by means of electrochemical impedance spectroscopy. These data allowed validating the use of the ionic liquid to measure the water diffusivity during inward and outward processes. The ionic liquid seem to play a positive role in the cathodic protection provided by the ZRP, as concluded from the current density and open circuit potential values. The observed improvement of the cathodic protection was attributed to the ionic liquid, which presence was confirmed through surface characterization techniques such as FTIR, SEM, EDX and XRF.

Keywords: Ionic liquids, zinc rich paints, water diffusivity, corrosion, electrochemical impedance spectroscopy, cathodic protection

Introduction

Over the last years, environmental concerns have highlighted the extensive and increasing importance of implementing more environmentally friendly and efficient industrial processes. In this sense, the emergence of ionic liquids has attracted a great scientific and industrial interest, due to their special properties such as their well-known negligible volatility,¹ which completely avoid air pollution typically associated to other conventional solvents, or their tunability, which eases the design of tailor-made solvents by combining cations and anions. This fact has led to their industrial application in some extant processes, so their annual production has already surpassed the tonne magnitude.² In particular, these molten salts have set the pace for the achievement of truly revolutionary processes in a diversity of fields: be it in biotechnology, analytical chemistry or electrochemistry.³ Within the latter, the use of ionic liquids for metal protection is a subject of particular importance and practical significance, since it may open up new opportunities in the field of corrosion inhibition.⁴⁻⁷

Since corrosion involves losses of millions dollars worldwide,⁸ the pursuit of more efficient protective methods is desired. Among the existing alternatives, epoxy coatings have been widely used in combination with other protective additives (e.g. zinc particles) in different kinds of corrosive environments. In this sense, metallic elements provide the

substrate with an additional cathodic protection which reinforces the inherent barrier properties associated to the epoxy coating.^{9,10} Nonetheless, corrosion products derived from zinc sacrificial protection could penetrate in the coating pores, thus reducing the duration of the cathodic protective effect. Several strategies have hitherto been proposed to improve the performance of zinc rich paints (ZRP), going from reducing the zinc particle size (from micro to nano scale) to the addition of nanoclays additives.^{9,11} Lately, Kowalczyk and Spychaj (2014) have demonstrated the beneficial effect of ionic liquids in the cathodic protection of ZRP, since they are hypothesized to further the electric contact between zinc particles, and also between them and the metallic substrate.¹²

Another advantage of ionic liquids is related to their good conductivity at room temperature promoting their application in electrochemistry as non-aqueous medium. In this line, the ease with which water and dissolved corrosive elements like NaCl are able to get through an specific protective coating is crucial for a proper evaluation of its resistance properties against corrosion.^{13,14} Among the available methods for studying water diffusion in coatings, electrochemical impedance spectroscopy (EIS) makes up the most appealing one, and was thus selected for the present work.^{15,16} Hence, the use of molten salts makes it possible to evaluate water uptake and desorption through subsequent wetting (in the presence of water) and drying (in the presence of ionic liquid) stages, respectively.

Taking into account the above mentioned, the ionic liquid 1-ethyl-3-methyl imidazolium ethylsulfate ($C_2C_1imC_2SO_4$) was selected for the first time to investigate the diffusivity of a model electrolyte (NaCl) in a ZRP, due to different advantages.

^a ENCOMAT Group, University of Vigo, 36310 Vigo, Spain. E-mail: mayren1980@uvigo.es, Tel.: +34 986 812213,

^b Department of Chemical Engineering, University of Vigo, 36310 Vigo, Spain

For instance, it displays a relatively low viscosity and melting point, a high thermal and chemical stability, and it is considered one of the cheapest molten salts, since it is already synthesized in a halide-free way at an industrial scale.¹⁷ The protective effects on a steel substrate, due to the addition of this imidazolium-based ionic liquid, were evaluated by means of EIS measurements for both constant immersion and cyclic tests. Nyquist and Bode diagrams were used to analyse the deterioration process of the epoxy layer. The aforementioned was also supported by potentiodynamic measurements performed on coated samples immersed in a 0.05M NaCl solution and in pure ionic liquid. Furthermore, several surface characterisation assays were employed to check the presence of the ionic liquid in the coated samples.

Materials and methods

Chemicals

The ionic liquid $C_2C_1imC_2SO_4$ was purchased from IoLiTec (purity higher than 99%), and its structure is shown in Fig. 1. Initially, it was subjected to vacuum drying ($P = 2 \cdot 10^{-1}$ Pa, $T = 313$ K) for several days in order to reduce moisture and possible solvents impurities. Besides, the ionic liquid was dried again after three cycles, in order to reduce the water content to a mass fraction lower than $2 \cdot 10^{-4}$, ascertained by means of a 756 Karl Fisher coulometer.

Insert Fig. 1

Colled rolled low carbon steel panels,¹⁸ with dimensions 150 mm x 100 mm x 1 mm and composed of Mn (0.05%), S (0.04%), C (0.12%) and P (0.04%) were the substrate for the ZRP. Possible organic compounds, salts, dust, etc. adhered to the steel samples were removed by the addition of detergent and high pressure fresh water. A surface profile corresponding to Rugotest No. 3 was carried out up to a Sa 2½.¹⁹ The corrosive process was stopped by placing the samples in an oven at 40°C, until the painting was carried out. A two-component, zinc rich epoxy primer cured with polyamide was applied by the air-less method, and was kindly donated by HEMPEL laboratories (Barcelona, Spain). After drying, they were kept in a desiccator until the beginning of the experiment. Thickness was determined by means of a digital coating thickness gauge (POSITECTOR®, Model 6000-1) where standards of 25, 250 and 1000 µm were used for calibration. The average thickness of the coated samples was 55 ± 5 µm.

Electrochemical Impedance Spectroscopy measurements

The experimental setup, shown in Fig. 2, consists of a glass circular tube, with an internal exposing area of 9.61 cm², fixed between two bakelite sheets joined by screws and isolated by a rubber seal (between glass/bakelite). The electrochemical cell includes the reference electrode (a platinum wire), the counter electrode (a platinum mesh), and the working electrode (the substrate). EIS measurements (by duplicate) were carried out by using a potentiostat Autolab® PGSTAT 30 (Eco Chemie) equipped with a frequency response analyser FRA module. Air humidity was avoided by performing the experimental measurements in a desiccator.

Constant immersion tests (IT) in the selected ionic liquid were carried out for 10 days to monitor impedance changes at open circuit potential every 6 h in the specimens (duplicate)

under study. The signal amplitude was 20 mV rms and the frequency ranged from 1 MHz down to 10 mHz.

Cyclic test (CT) consisted of two subsequent stages (one cycle) of 24 hours in 0.05 M NaCl solution (wetting stage, W) and 24 h in $C_2C_1imC_2SO_4$ (drying stage, D). This procedure was repeated 7 times (cycles) for the painted specimens. The electrochemical cell was disassembled and cleaned with distilled water after each immersion. Every 40 min EIS data were collected at the same frequency range and signal amplitude used for those defined for the IT.

Insert Fig. 2

Polarization curves

Cathodic and anodic polarization curves were carried out in the potential range of ± 300 mV in relation to E_{ocp} (open circuit potential) at the scan rate of 1 mV/s. The corrosion potential (E_{corr}), the corrosion current density (i_{corr}) and the corrosion rate (CR) were obtained from the Tafel straight lines by using the electrochemical software (GPES). Potentiodynamic scans were carried out at 2, 24 and 72 h of immersion of the coated samples in the ionic liquid and in the NaCl solution.

Surface characterization

Morphology and composition of specimens under investigation were obtained with SEM and EDX assays by using a FE-SEM JEOL JSM6700F model with an energy dispersive X-ray detector EDS Oxford Inca Energy 300. Attenuated Total Reflectance Fourier Transform Infrared Spectroscopy (ATR-FTIR) test was carried out in a Nicolet 6700 spectrometer using a KBr beamsplitter and an DTGS KBr detector in the range from 400 cm⁻¹ to 4000 cm⁻¹. Also, X-ray fluorescence (XRF) tests were performed in a Siemens SRS3000 XRF sequential X-ray spectrometer.

Ionic liquid recycling

The density of the ionic liquid was determined with an Anton Paar DSA -5000 digital vibrating tube densimeter, and this property served as a tool to check the viability of ionic liquid recycling. The apparatus was calibrated by measuring the density of Millipore quality water and ambient air according to manual instructions, and the quality of the calibration was checked by comparing the density of well-known pure liquids. The repeatability and uncertainty in the experimental measurements (as defined by the manufacturer) have been found to be lower than $\pm 2 \cdot 10^{-6}$ and $\pm 10^{-5}$ g/cm³, respectively.

Results and discussion

Analysis of coating performance by EIS data

A deep analysis of the impedance spectra obtained from the EIS measurements constitutes a valuable piece of information for understanding the anticorrosive properties and the kinetics of the corrosion process in protective coatings.

The first step of the work consists of evaluating the electrochemical behaviour of the ZRP in the presence of $C_2C_1imC_2SO_4$. This ionic liquid will be used for determining the coating behaviour during CT, since it allows determining water diffusivity parameters in subsequent wetting (0.05 M of NaCl) and drying cycles (ionic liquid). For comparative

purposes the coating performance under 0.05 M of NaCl solution was also studied by EIS measurements.

Immersion Test of the ZRP in 0.05 M NaCl solution

The evolution over time of the impedance diagrams obtained for the samples immersed in 0.05 M NaCl solution are shown in Fig. 3. At the beginning of the experiment, high impedance values (around $130 \cdot 10^6 \text{ ohm} \cdot \text{cm}^2$) at the low frequency domain are noticed (Fig. 3A). This is in agreement with the high frequency loop and the high impedance modulus value recorded in Fig. 3C, typically detected in an intact paint. In relation with this, two time constants can be observed at initial time, which should be related with the typical response observed for both the zinc native oxide layer and the resin in a ZRP (which behaves as a dielectric layer), as suggested by Abreu *et al.*²⁰ Then, as time goes by, the impedance continues decreasing to $250 \cdot 10^3 \text{ ohm} \cdot \text{cm}^2$ approximately at the end of the experiment (240 h). At this time, two loops at high and middle frequency, and probably a third one at low frequency (not clearly defined) are visualized (Fig. 3B, 240 h). In line with previous investigations,^{20,21,22} the insulating properties of the paint, the electrochemical double layer and the diffusion process are associated with the first, second and third time constant, respectively. The emergence of a third time constant indicates that the cathodic protection has started to disappear, so the corrosion protection is only based on a barrier effect.

Insert Fig. 3

Immersion Tests of the ZRP in ionic liquid

The impedance spectra of the coated specimens immersed in the ionic liquid are depicted in Fig. 4 where a high impedance value (around $60 \cdot 10^6 \text{ ohm} \cdot \text{cm}^2$) is observed from the beginning of the experiment (0 h). Then, from 6 to 90 h of immersion in the ionic liquid, a continuous diminution of impedance was evidenced, in line with the trends observed for the same system in the presence of 0.05 M NaCl solution. However, it is interesting to notice how the impedance increased nearly twice (almost the double) from 90 h on, reaching about $1.2 \cdot 10^6 \text{ ohm} \cdot \text{cm}^2$ (Fig. 4B). The previously mentioned is supported by the capacitive loop observed at high frequency and the high impedance modulus reached (around $\text{Mohm} \cdot \text{cm}^2$) at this time (240 h), indicating the better protective properties of the ZRP exposed to the ionic liquid. Additionally, two time constants located at the high and low frequency domain can be depicted from 0 h to 90 h of immersion, related to the dielectric properties of the film and the double layer, as stated before. On the other hand, from 90 h on, the impedance increases continuously and the same two time constants are depicted. This behavior points that the galvanic protection mechanism is still active, probably due to the beneficial effect of the presence of the ionic liquid, contrarily to the conclusions reported for panels in 0.05 M NaCl solution.

Insert Fig. 4

Cyclic Tests

Then, from the EIS data in CT, the capacitance evolution (C) for the wetting and drying stages was calculated as follows:

$$C = (-\omega Z_i)^{-1} \quad (1)$$

being ω the angular frequency and Z_i the imaginary impedance values at 10 kHz in the EIS measurements

performed every 40 min. The values obtained for wetting and drying stages are represented in Fig. 5A and B, respectively. Generally speaking, the Fig. 5A reveals an initial linear increase in the capacitance values prior to the stabilization in a steady state, indicating the saturation of the coating, thus leading to stable values of capacitance. On the one hand, it is noticeable that in the first cycles (1A and 2A) a maximum in the capacitance values is reached, which is not typical for a second order Fick-type evolution.²³ This anomaly has already been observed in previous research works, and might be indicative of water accumulation at the coating-metal interface.^{24,25}

Insert Fig. 5

On the other hand, when the number of cycles is increased, a second order Fickian-type trend is observed, maybe as a consequence of the plasticization of the epoxy coating. It is also interesting to note that, generally, the more cycles are run, the higher levels of capacitance are reached. However, some exceptions can be remarked for cycles 3A, 4A, 6A and 7A, probably as a consequence of the formation of preferential routes within the ZRP.

Similarly, the behavior for the drying stage (Fig. 5B) fits well to the Fick's second law, with an initial linear decreased capacitance as the time is increased until a constant value, which reveals the end of water desorption of the ZRP. In this case, the trends are the same regardless of the cycle under study. The obtained results confirm the suitability of the selected ionic liquid to be used as non-aqueous medium in order to study the water outward diffusion in this kind of coatings.

Analysis of diffusivity

Once the viability of the selected $\text{C}_2\text{C}_{1\text{im}}\text{C}_2\text{SO}_4$ as non-aqueous medium was demonstrated through both IT and CT, the diffusion coefficients for the wetting (D_{in}) and drying (D_{out}) stages were ascertained as follows:

$$\frac{\frac{\log Ct}{C_0}}{\frac{\log Cs}{C_0}} = \sqrt{\frac{4Dt}{L^2\pi}} \quad (2)$$

being C_0 the initial capacitance, C_t the capacitance at time (t), C_s the saturation capacitance, and L the thickness of the layer ($55 \pm 5 \mu\text{m}$). From the linearization of this expression, the diffusion coefficients were calculated, and the values obtained are listed in Table 1, together the regression coefficients of the fittings and the required relevant parameters.

Insert Table 1

For a better analysis of the diffusivity data, D_{in} and D_{out} have been plotted in Fig. 6 versus the 7 cycles investigated. In a visual inspection of the data it is possible to conclude that water molecules diffuse outwards at lower rates than during the uptake (average $D_{\text{out}} = 3.10 \cdot 10^{-13} \text{ m}^2 \text{ s}^{-1}$ and average $D_{\text{in}} = 5.45 \cdot 10^{-13} \text{ m}^2 \text{ s}^{-1}$) in agreement with previous studies.²⁵ Besides, the lower values of diffusivity are recorded in the first cycle, which could be motivated by the typical barrier effect faced for an intact coating. Then, D_{in} increased from the first to the second cycle in more than 3 folds, an effect probably due to the above mentioned formation of preferential channels inside the coating favoring water uptake. The fluctuations recorded for the following cycles may be associated with the presence of zinc corrosion products plugging ZRP pores. Additionally, the

interaction of hydroxyl groups existing in the zinc-rich epoxy coating with water molecules should also be taken into account to explain the differences obtained in the diffusivity values of water uptake. Regarding D_{out} values, no important alterations are observed in the figure, except for the first cycle, where the barrier effect is more remarkable.

Insert Fig. 6

Polarization curves

In order to get further insight into the electrochemical performance in the presence of the selected ionic liquid, the potentiodynamic polarization curves at 2, 24 and 72 h are presented in Fig. 7.

Insert Fig. 7

These data reveal a close resemblance in curves morphology for all the immersion times and for both electrolyte conditions (NaCl 0.05 M and ionic liquid). It is also noticeable that the studied systems are controlled by electron transfer, and the apparent similarity of the slopes of the anodic and cathodic branches suggest the existence of a mixed control. On the other hand, it becomes patent that higher values of current density are reached as immersion time is increased, no matter the electrolytic medium under investigation. Additionally, the comparison between NaCl and ionic liquid reveals that slightly lower levels of current density are recorded for the latter. This statement is corroborated when the Tafel experimental data, listed in Table 2, are analysed. Thus, the lowest value of i_{corr} and CR was obtained for the system after 2 h in the presence of $\text{C}_2\text{C}_1\text{imC}_2\text{SO}_4$, with $1.22 \cdot 10^{-9}$ A/cm² and $1.31 \cdot 10^{-7}$ mm/year, respectively, while the system immersed in NaCl 0.05M for the same time led to $1.30 \cdot 10^{-9}$ A/cm² and $1.40 \cdot 10^{-7}$ mm/year, respectively. This behaviour is confirmed after 24 h of immersion.

Insert Table 2

Regarding the open circuit potential (OCP), the data shown in Fig. 7 evidences an opposite trend for the systems in the molten salt and those in the NaCl 0.05 M. Thus, while the steel/ZRP/ionic liquid systems tend to more positive values as time is increased, the steel/ZRP/NaCl specimens tend to reduced open circuit potential values. It is also noticeable how the OCP values for the former system are always more active (more negative) than the same system immersed in a NaCl solution. Hence, these data allow concluding that the selected ionic liquid probably promotes the activation of the zinc pigments for longer times, extending the duration of the cathodic anticorrosive protection. This is in agreement with the impedance values attained, since a greater anticorrosive resistance of the ZRP in contact with the ionic liquid was checked.

Surface characterization

The aim of surface characterization analysis is to demonstrate the possible presence of $\text{C}_2\text{C}_1\text{imC}_2\text{SO}_4$ inside the coated samples after being tested in IT and CT, respectively. At first, it is important to know the main components in a ZRP which are an organic epoxy resin (contains carbon and hydrogen) and zinc pigments; even though negligible amounts of other elements such as nitrogen, magnesium, aluminium, silicon, sulfur, etc. can also be present.

SEM images of the frontal view of the painted specimens (reference and tested) evidenced no relevant morphological changes between them (Fig. 8A and B). However, EDX spectrum of the reference sample indicates that sulfur was not present (Fig. 8A), and only the main constituents of the ZRP have been detected, contrarily to what happens for the sample submitted to 10 days of constant immersion in the ionic liquid (Fig. 8B), which reveals that some rests of the molten salt could remain in the paint after IT.

Insert Fig. 8

From ATR-FTIR data (Fig. 9) no important differences were visualized between the transmittance spectra of the reference and tested samples. The main functional groups detected are specific for an epoxy resin which are OH and NH ($3200\text{-}3500$ cm⁻¹), CH aromatic ($3000\text{-}3100$ cm⁻¹), CH aliphatic ($2700\text{-}3000$ cm⁻¹); CO amide (1650 cm⁻¹), C-C aromatic (1600 cm⁻¹), *p*-substituted benzene (1500 cm⁻¹), C-O secondary alcohol (1190 cm⁻¹), CO aromatic (1040 cm⁻¹), out of plane bending of aromatic C-H (840 cm⁻¹) and out of plane ring C-C bend (560 cm⁻¹), in agreement with a previous study.¹⁴

Insert Fig. 9

However, some technical limitations during measurement (lack of contact between the sample and the ATR crystal due to the porous nature of the former) could hinder an appropriate analysis. Hence, a very suitable technique for sulfur detection such as XRF was employed. Results confirm the presence of this element in all samples (reference and tested samples) which was not seen in previous evaluations of the reference ones (see Table 3). Additionally, a notable increment of sulfur from the reference to the tested samples (around 2 times higher) proves the presence of the ionic liquid and confirms the hypothesis that the molten salt is exerting a beneficial anticorrosive role on the ZRP-coated specimens.

Insert Table 3

It should be noted that $\text{C}_2\text{C}_1\text{imC}_2\text{SO}_4$ was recovered after IT and CT, and the analysis of its density at different temperatures reveal differences lower than 1% (1.29167 g/mL for the ionic liquid prior to the experiment, and 1.28094 g/mL after the experiment, at 25°C). This confirms the high stability of the ionic liquid after being exposed to 0.05 M NaCl solution for 7 cycles (CT) and also in contact with the ZRP, which makes it possible to reuse it for further experiments.

Conclusions

Preliminary research findings obtained have proved that the use of the ionic liquid $\text{C}_2\text{C}_1\text{imC}_2\text{SO}_4$ improves the cathodic protection of ZRP. Impedance results indicated that the samples exposed to the molten salt have higher impedance values and only two time constants, suggesting that the zinc sacrificial protection is still active. Polarization tests revealed that the most negative OCP values were reported for panels exposed to the ionic liquid, which points out the extension of the cathodic anticorrosive protection duration. It was also demonstrated the suitability of the ionic liquid for studying inward and outward diffusion process as well as for determining diffusivity parameters.

Surface characterization allowed concluding that there is no morphological change (by SEM) in the tested samples exposed to the ionic liquid. However, XRF data evidenced the presence of sulfur (by XRF) in both reference and tested panels, but the

highest content was detected in ZRP samples immersed in the ionic liquid for several days, thus confirming that the positive effects observed in the coating are due to the presence of the molten salt. However, further studies at longer immersion times are necessary in order to shed light on the electrochemical mechanism underlying the behaviour of the selected ionic liquid in the ZRP.

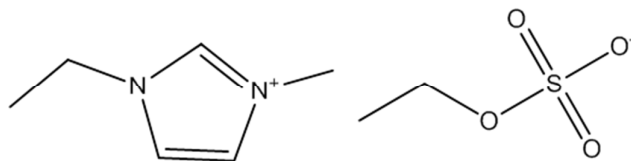
Acknowledgements

M. Echeverría is very grateful to the University of Vigo for funding through a PhD grant and to the ENCOMAT group (University of Vigo) for its valuable support. The authors acknowledge Spanish Ministry of Economy and EDERF funds and Competitiveness for funding through CTM2012-31534 project. The authors also thank the important support of HEMPEL laboratories (Barcelona, Spain) and CACTI (Center for Scientific and Technological support) at the University of Vigo, for the supply of coatings and samples preparation and their valuable assistance with FTIR and XRF measurements, respectively.

References

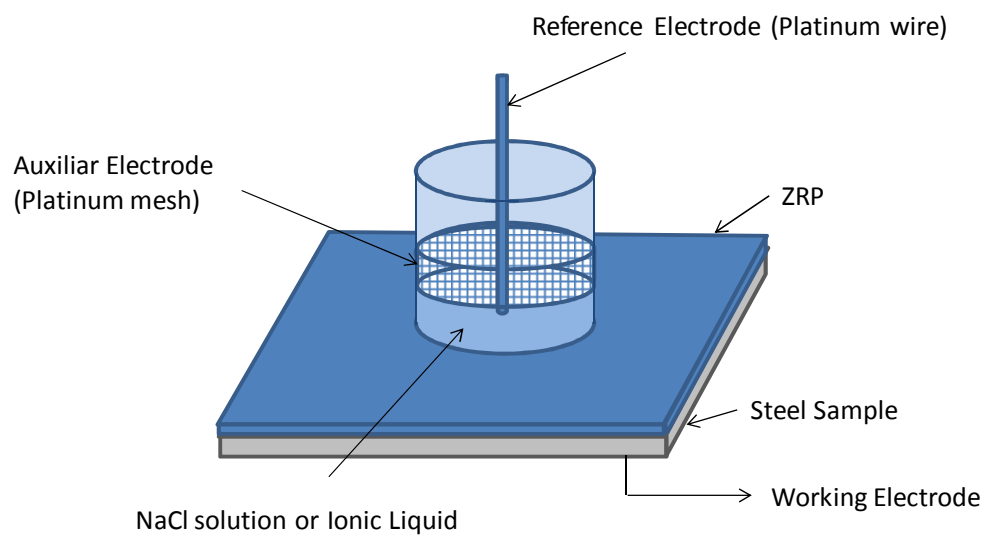
- M. J. Earle, J. M. S. S. Esperança, M. A. Gilea, J. N. Canongia Lopes, L. P. N. Rebelo, J. W. Magee, K. R. Seddon and J. A. Widegren, *Nature*, 2006, **439**, 831-834.
- F. J. Deive, A. Rodríguez, A. Varela, C. Rodrigues, M. C. Leitão, J. A. M. P. Houbraken, A. B. Pereiro, M. A. Longo, M. A. Sanromán, R. A. Samson, L. P. N. Rebelo and C. Silva Pereira, *Green Chem.* 2011, **13**, 687-696.
- N. V. Plechkova and K. R. Seddon, *Chem. Soc. Rev.* 2008, **37**, 123-150.
- T. Tüken, F. Demir, N. Kıcı, G. Sıgırcık, and M. Erbil, *Corrosion Sci.*, 2012, **59**, 110-118.
- N. Likhonova, M. Domínguez-Aquilar, O. Olivares-Xometl, N. Nava-Entzana, E. Arce, and H. Dorantes, *Corrosion Sci.*, 2010, **52**, 2088-2097.
- X. Zhou, H. Yang and F. Wang, *Electrochim. Acta*, 2011, **56**, 4268-4275.
- H. Ashassi-Sorkhabi and M. Es'haghi, *Mater. Chem. Phys.*, 2009, **114**, 267-271.
- M. Echeverría, C. M. Abreu, C. A. Echeverría. Assessing pretreatment effect on the protective properties of different coating systems against marine corrosion. *Corrosion* 2014. Preprint. <http://dx.doi.org/10.5006/1278>.
- K. Schaefer and A. Miszczyk. *Corrosion. Sci.*, 2013, **66**, 380-391.
- N. Hammouda, H. Chadli, G. Guillemot, K. Belmokre, The Corrosion Protection Behaviour of Zinc Rich Epoxy Paint in 3% NaCl Solution, *Adv. Chem. Engineer. Sci.*, 2011, **1**, 51-60.
- N. Arianpouya, M. Shishesaz and A. Ashrafi, *Surf. Coat. Technol.*, 2013, **216**, 199-206.
- K. Kowalczyk and S. Szychaj, *Corrosion Sci.*, 2014, **78**, 111-120.
- R. M. Souto, Y. González-García, J. Izquierdo and S. González, *Corrosion Sci.*, 2010, **52**, 748-753.
- F. Contu, L. Fenzy and S. R. Taylor, *Prog. Org. Coat.*, 2012, **75**, 92-96.
- N. Fredj, S. Cohendoz, S. Mallarino, X. Feaugas and S. Touzain, *Prog. Org. Coat.*, 2010, **67**, 287-295.
- S. Shreepathi, S. M. Naik and M. R. Vattipalli, *J. Coat. Technol. Res.*, 2012, **9**, 411-422.
- A. B. Pereiro, F. J. Deive, J. M. S. S. Esperança and A. Rodríguez, *Fluid Phase Equilib.*, 2010, **291**, 13-17.
- UNE-EN 10130, "Productos planos laminados en frío de acero bajo en carbono para embutición o conformación en frío - Condiciones técnicas de suministro" (Madrid, Spain: Spanish Standardization and Certification Association [AENOR], 2008).
- UNE-EN ISO 8501-1, "Preparación de substratos de acero previa a la aplicación de pinturas y productos relacionados - Evaluación visual de la limpieza de las superficies - Parte 1: Grados de óxido y de preparación de substratos de acero no pintados después de eliminar totalmente los recubrimientos anteriores" (Madrid, Spain: Spanish Standardization and Certification Association [AENOR], 2008).
- C. M. Abreu, M. Izquierdo, M. Keddah, X. R. Nóvoa, and H. Takenouti, *Electrochim. Acta.*, 1996, **41**, 240-2415.
- J. R. Vilche, E. C. Bucharsky and C. A. Giúdice, *Corrosion Sci.*, 2002, **44**, 1287-1309.
- Ji Hoon. Park, Tea Ho. Yun, Kyoo Young. Kim, Yon Kyun. Song and Jong Myung. Park, *Prog. Org. Coat.*, 2012, **74**, 25-35.
- F. Deflorian, L. Fedrizzi, S. Rossi and P. L. Bonora, *Electrochim. Acta.*, 1999, **44**, 4243-4249.
- K. N. Allahar, B. R. Hinderliter, G. P. Bierwagen, D. E. Tallman and S. G. Croll, *Prog. Org. Coat.*, 2008, **62**, 87-95.
- K. N. Allahar, B. R. Hinderliter, A. M. Simoes, D. E. Tallman, G. P. Bierwagen and S. G. Crolla, *J. Electrochem. Soc.*, 2007, **154**, F177-F185.

1 **Fig. 1** Structure of 1-ethyl-3-methyl imidazolium ethylsulfate ionic liquid.



2
3
4
5
6
7
8
9
10
11

12 **Fig. 2** Setup of the electrochemical cell used for EIS measurements.



13

14

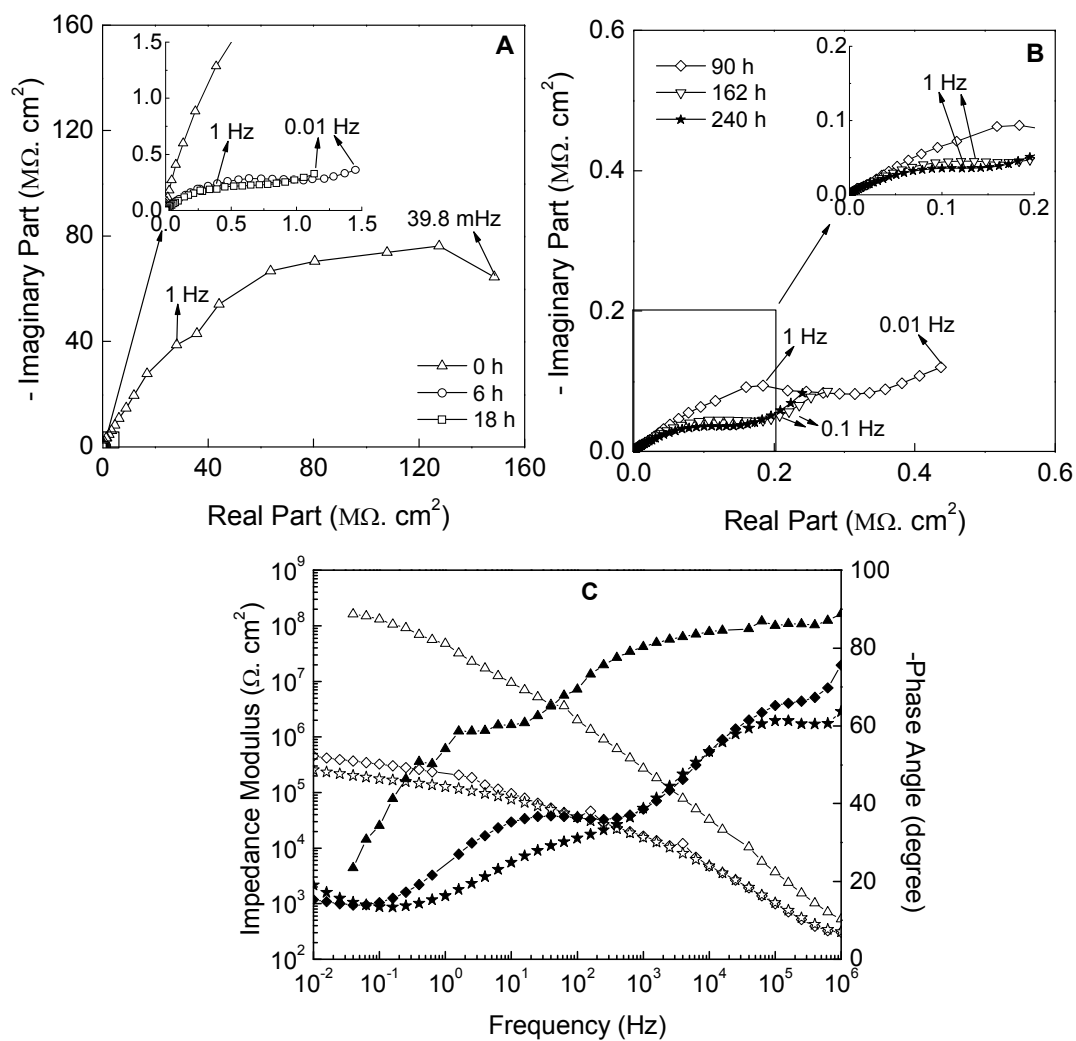
15

16

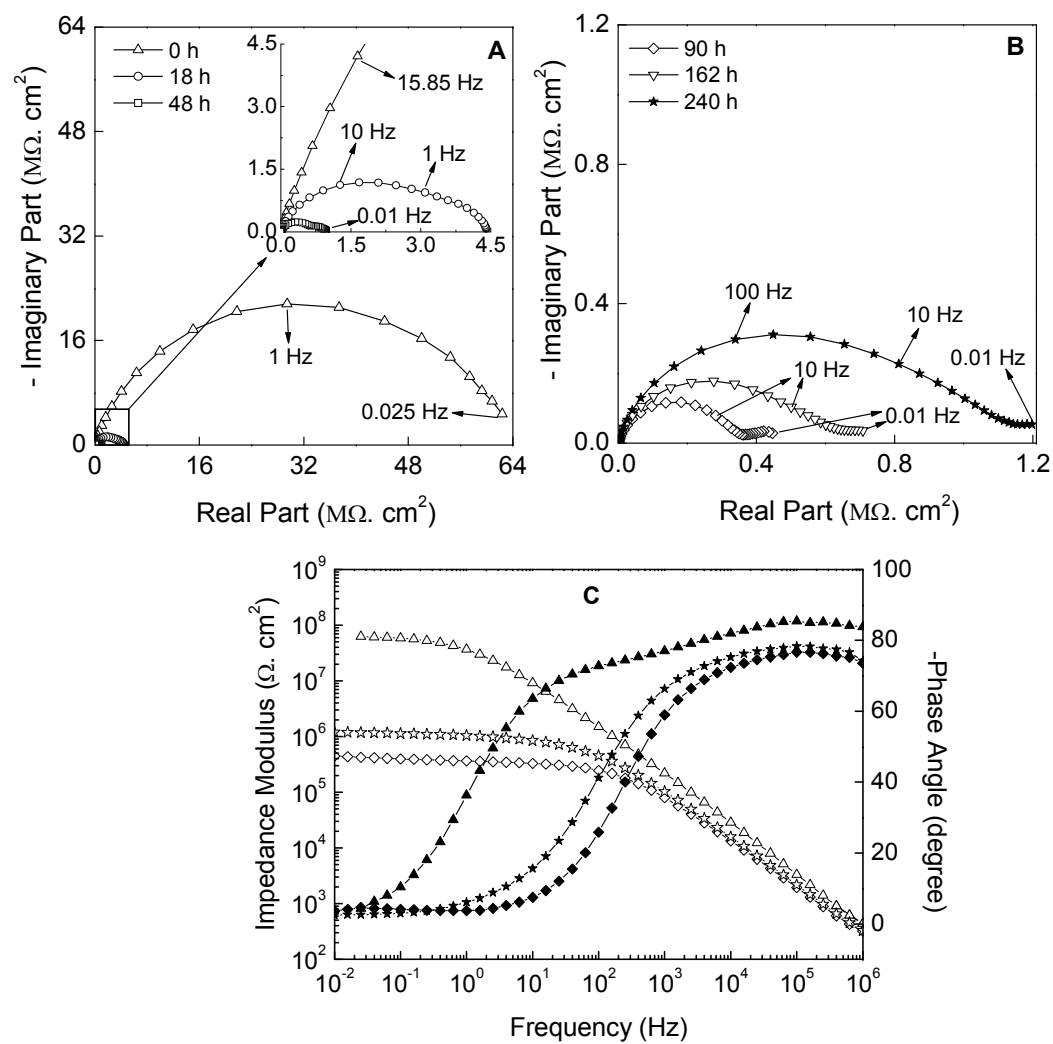
17

18 **Fig. 3** Impedance spectra of the ZRP in the presence of 0.05 M NaCl solution. Nyquist plots are represented at A) 0 h (Δ), 6 h (\circ), 18 h (\square), B) 90 h (\diamond), 162 h (∇) and 240 h ($*$) and bode plots at C) 0 h (Δ), 90 h (\diamond) and 240 h ($*$) where the full symbols represent the phase angle and the empty ones the impedance modulus.

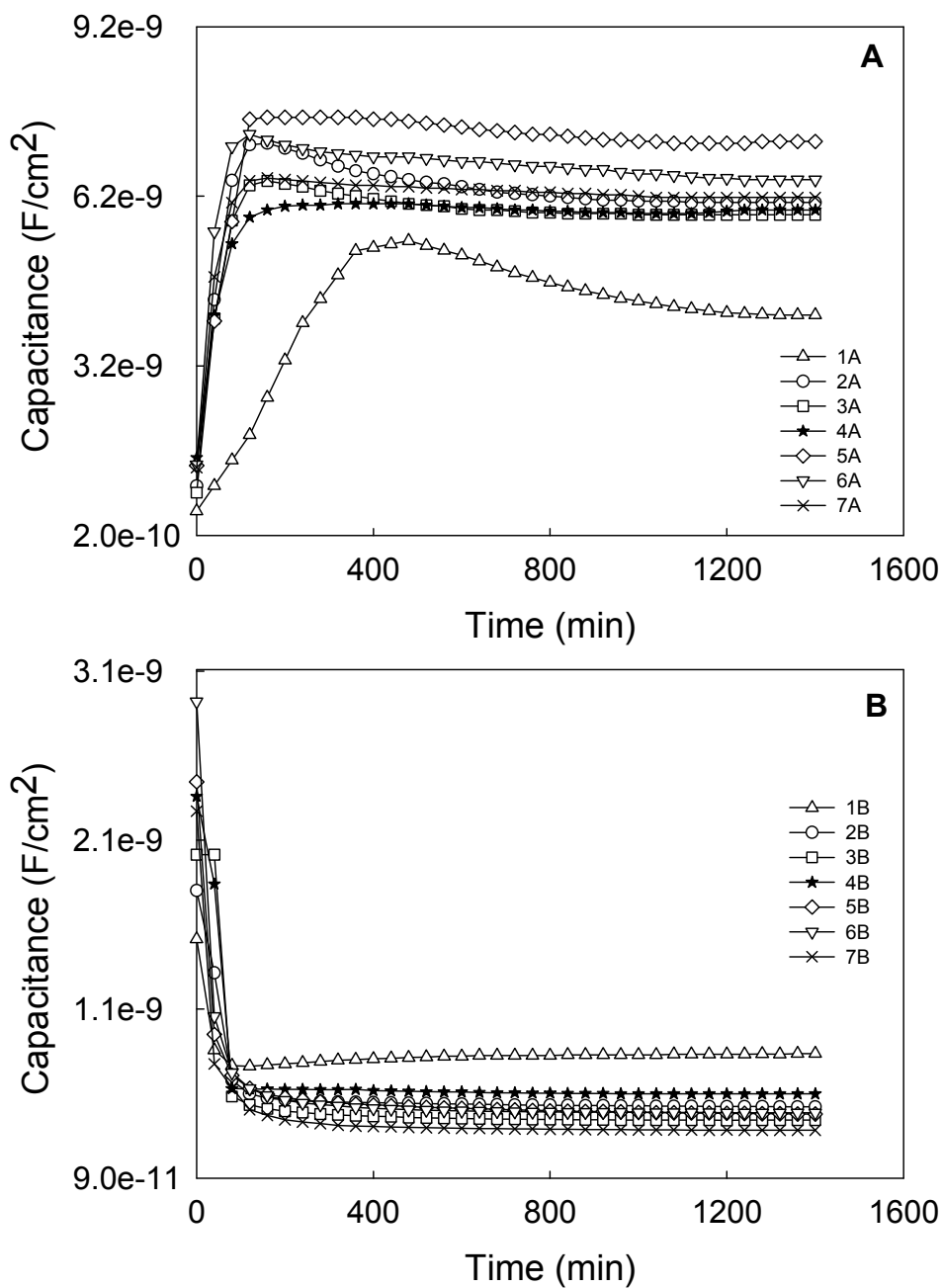
19
20
21



22 **Fig. 4** Impedance diagrams of the ZRP in the presence of the ionic liquid. Nyquist plots are represented at A) 0 h (Δ), 18 h (\circ), 48 h (\square), B) 90 h (\diamond), 162 h (∇)
 23 and 240 h ($*$) and bode plots at C) 0 h (Δ), 90 h (\diamond) and 240 h ($*$) where the full symbols represent the phase angle and the empty ones the impedance
 24 modulus.
 25

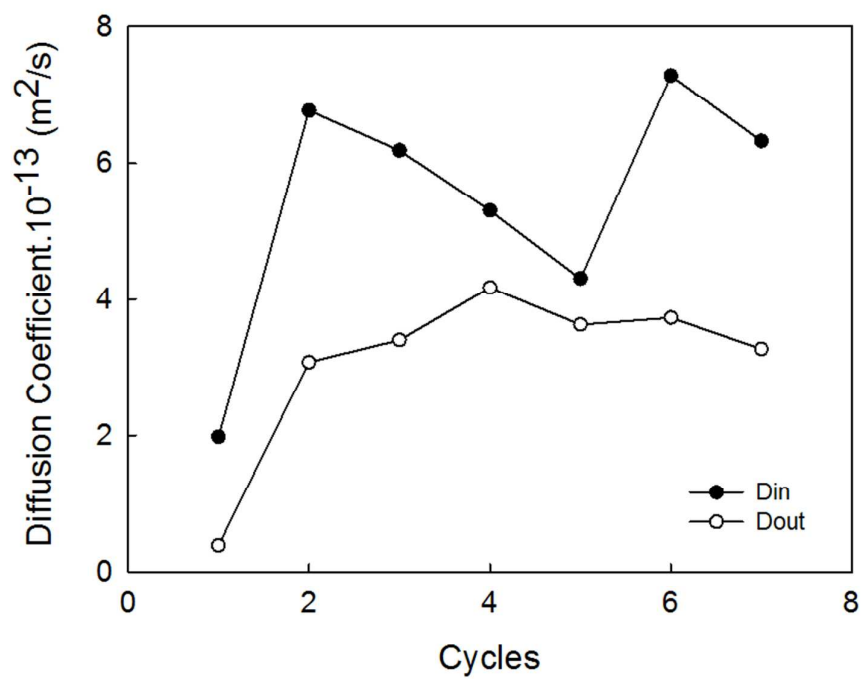


26 **Fig. 5** Capacitance evolution (10 KHz) vs. time of the coated sample exposed to 7 experimental
27 cycles of continuous wetting (A) and drying (B) periods for CT.
28



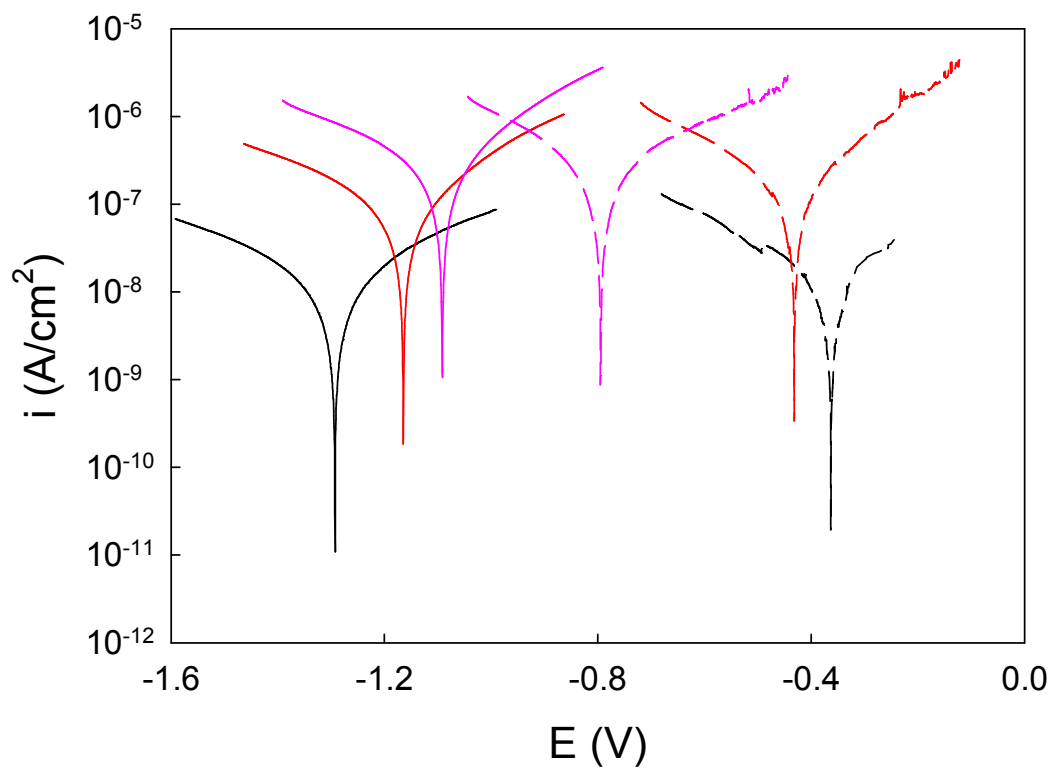
29

30 **Fig. 6** Evolution of the diffusion coefficient of the ZRP vs. experimental cycles of continuous
31 wetting (D_{in}) and drying (D_{out}).
32
33



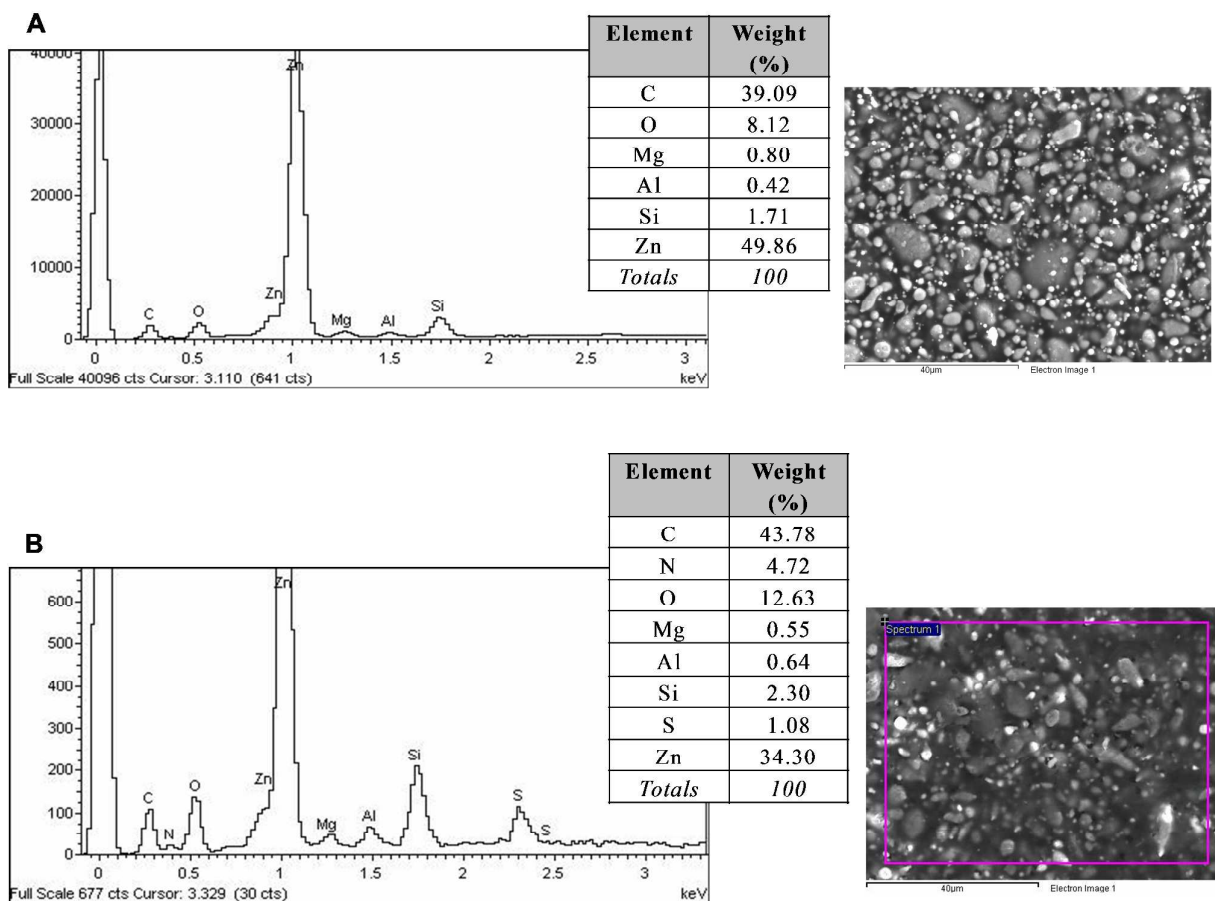
34
35
36
37

38 **Fig. 7** Polarization curves obtained for the steel/PRZ system after being continuously immersed
39 (2, 24 and 72 h) in 0.05 M NaCl solution (dashed lines) and in $C_{2}C_{1}imC_{2}SO_{4}$ (solid lines).
40 Black, 2 h; Red, 24 h; Pink 72 h.



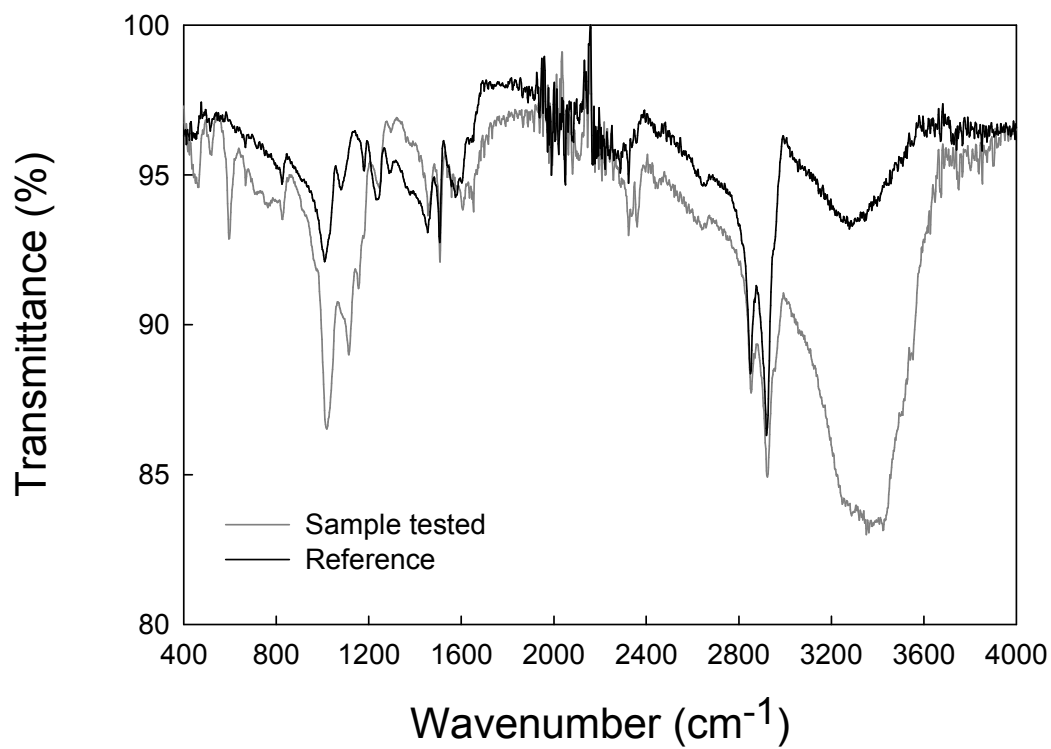
41
42

43 **Fig. 8** SEM images and EDX spectra of the ZRP panels (frontal view): A) before (reference
 44 sample - without ionic liquid) and B) after (tested sample - exposed to the ionic liquid) being
 45 immersed 10 days in the ionic liquid.
 46



47
 48

49 **Fig. 9** Transmittance spectrum of the ZRP after a 10-days immersion test in the ionic liquid.
50 Comparison spectra between reference (without ionic liquid) and sample tested (exposed to
51 ionic liquid).



52
53
54
55

1

Table 1 Parameters used for the calculation of the diffusion coefficients for wetting (A) and drying (B) stages in CT

Cycles	Co (nF)	Cs(nF)	Slope (Fs ^{-0.5})	D·10 ⁻¹³ (m ² s ⁻¹)	R ²
1A	6.08	39.41	0.007	1.98	0.99
1B	14.47	0.83	-0.005	0.38	0.98
2A	10.33	58.51	0.012	6.77	0.99
2B	17.22	4.93	-0.006	3.08	0.82
3A	9.20	56.44	0.012	6.19	0.99
3B	19.26	4.17	-0.007	3.40	0.99
4A	15.16	57.25	0.008	5.30	0.99
4B	22.58	5.66	-0.007	4.17	0.70
5A	13.81	68.90	0.009	4.31	1.00
5B	23.41	4.60	-0.008	3.63	1.00
6A	13.96	62.41	0.010	7.28	0.98
6B	27.96	4.59	-0.009	3.73	1.00
7A	13.49	59.39	0.010	6.32	0.98
7B	21.73	3.59	-0.008	3.27	0.98

2

3

Table 2 Main parameters calculated by Tafel test for the system steel/PRZ after continuous immersion in NaCl 0.05 M solution and ionic liquid

Electrolyte	Immersion time (h)	E_{corr} (mV*)	i_{corr} (A/cm ²)	CR (mm/year)
0.05 M NaCl solution	2	-365	$1.30 \cdot 10^{-9}$	$1.40 \cdot 10^{-7}$
	24	-432	$1.24 \cdot 10^{-8}$	$1.34 \cdot 10^{-6}$
	72	-795	$2.65 \cdot 10^{-8}$	$2.75 \cdot 10^{-6}$
C ₂ C ₁ imC ₂ SO ₄	2	-1292	$1.22 \cdot 10^{-9}$	$1.31 \cdot 10^{-7}$
	24	-1165	$8.25 \cdot 10^{-9}$	$8.89 \cdot 10^{-7}$
	72	-1092	$2.55 \cdot 10^{-8}$	$2.86 \cdot 10^{-6}$

4

* vs. Platinum reference electrode

5 **Table 3** Chemical elements detected in the reference and the tested samples after X-ray
6 fluorescence test

Formula	Reference (%)	Tested Sample* (%)
Mg	2.90 +/- 0.05	3.2 +/- 0.07
Al	2.90 +/- 0.38	3.6 +/- 0.49
Si	8.00 +/- 0.23	8.7 +/- 0.21
S	0.77 +/- 0.88	2.9 +/- 0.99
Cl	2.20 +/- 0.12	2.2 +/- 0.14
K	0.45 +/- 0.02	0.41 +/- 0.04
Ca	0.52 +/- 0.70	0.7 +/- 0.11
Fe	0.91 +/- 0.25	1.01 +/- 0.37
Zn	81.43 +/- 1.40	77.29 +/- 1.39

7 *after 10 days of IT in the ionic liquid

7

8

9